

Electrostatically modulated magnetophoretic transport of functionalised iron-oxide nanoparticles through hydrated networks

Stephen Lyons,^a Eoin P. McKiernan,^b Garret Dee,^c Dermot F. Brougham,^{b*} and Aoife Morrin^{a*}

^a Insight SFI Research Centre For Data Analytics; National Centre for Sensor Research; School of Chemical Sciences, Dublin City University, Ireland.

^b School of Chemistry, University College Dublin, Ireland.

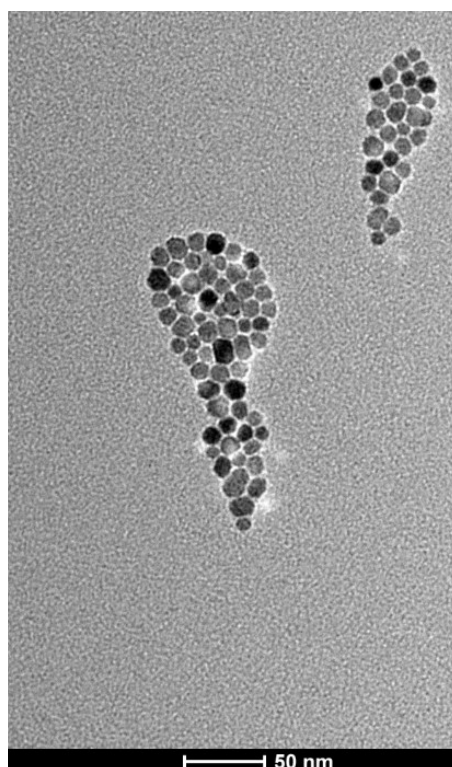


Figure S1 TEM image of synthesised MNPs at 150k magnification. d_{hyd} was measured from these images using Image J and found to be 8.9 ± 0.8 nm ($n=205$).

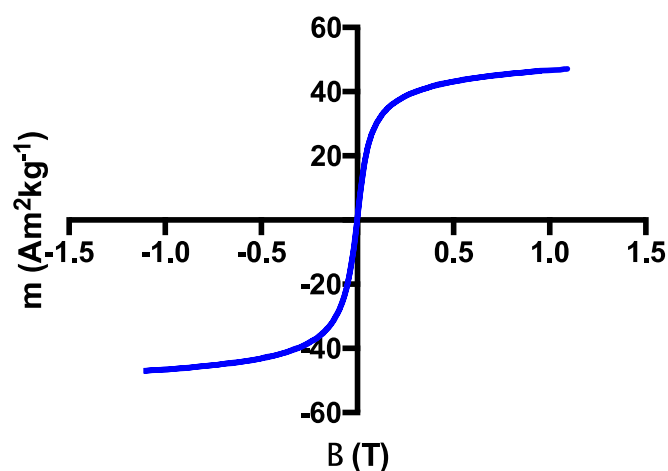


Figure S2 Magnetometry data, recorded at 298 K for dried the synthesised MNP cores. The data shows effectively zero coercivity ($M=0$ at $H=0$) field, confirming that the MNPs are superparamagnetic. χ_v (equation 1) is calculated as 0.289 from ratio of M/B for $B = 0.23$ T, which corresponds to 6.0 mm distance from the magnet,¹ *i.e.* at the top of each gel.

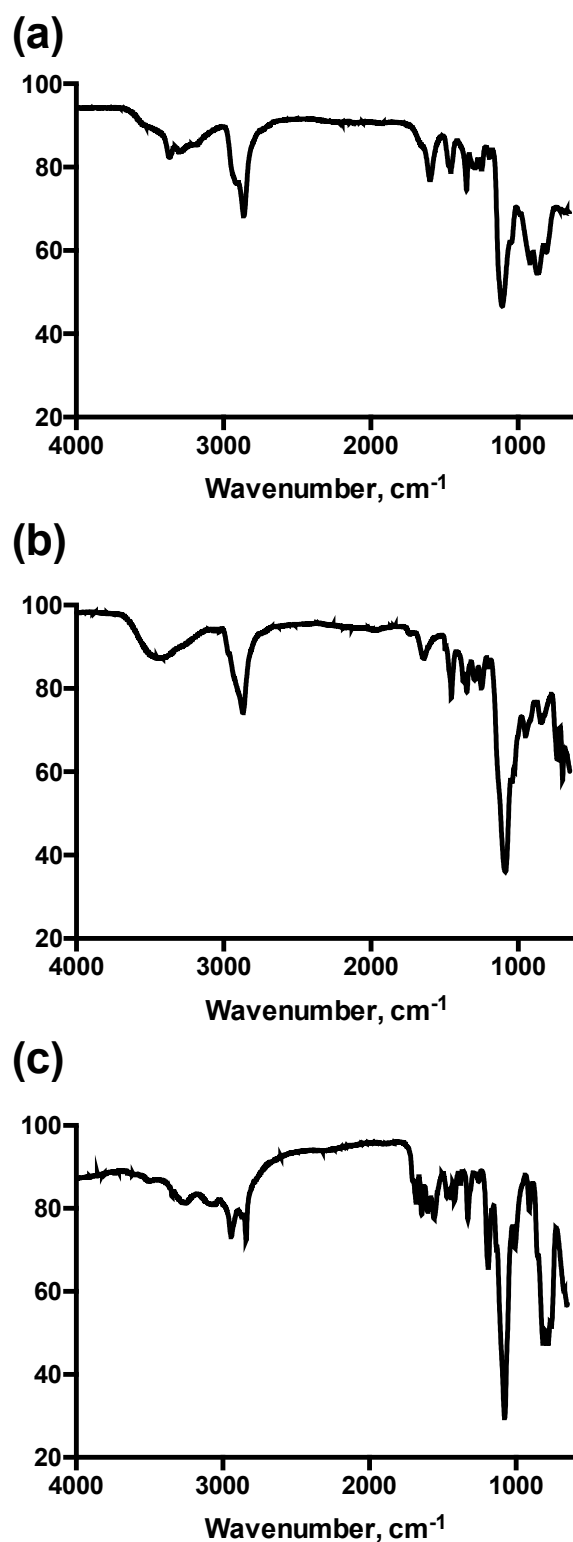


Figure S3. FTIR spectra of (a) GLYMO-MNPs, (b) PEG1000-MNPs, (c) arginine-MNPs.

The GLYMO-MNPs exhibit Si–O, Si–O–R stretching modes at 1107 and 1052 cm^{-1} , respectively, in addition to the C–H asymmetric stretching modes at 2861 cm^{-1} . The most notable features of the GLYMO-MNPs are the epoxide ring modes at 864, 916 and 1295

cm^{-1} , which were not observed after the coupling reactions. The PEG1000-MNPs exhibit Si–O stretching modes at 1088 cm^{-1} , respectively, in addition to the C-H asymmetric stretching modes at 2869 cm^{-1} . After the epoxide ring has been broken, the associated C-N stretching and N-H bending modes were observed in the region of 1643 cm^{-1} . C–O–C stretching vibrations were observed in region of $1043\text{--}1080\text{ cm}^{-1}$. The arginine-MNPs exhibit Si–O stretching modes at 1077 cm^{-1} , respectively, in addition to the C-H asymmetric stretching modes at 2841 cm^{-1} . The characteristic N-H and N=H stretching modes can be seen in the region of $1680\text{--}1543\text{ cm}^{-1}$. An O-H stretch is also seen at 2942 cm^{-1} , while C-O-C stretches are seen in the region of 1450 cm^{-1} .

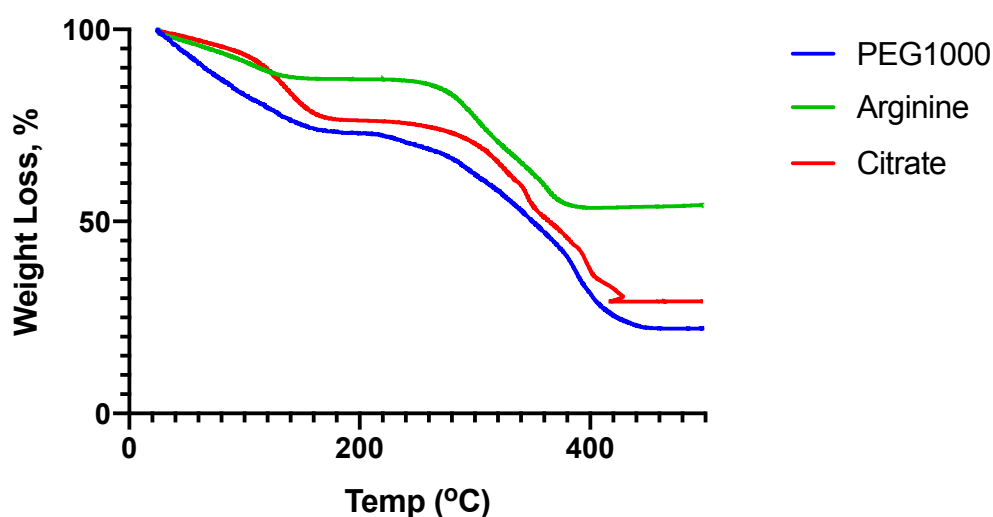


Figure S4 TGA of PEG1000-MNPs (Grafting density 1.99 nm^{-2}), arginine-MNPs (Grafting density 0.77 nm^{-2}) and citrate-MNPs (Grafting density 1.79 nm^{-2}). Grafting density values calculated are consistent with the literature^{2,3}.

Two-step weight loss is seen for both PEG- and arginine-MNPs, initial loss is due to water molecules decomposing at $80\text{--}130^\circ\text{C}$. The second weight drop seen at $280\text{--}400^\circ\text{C}$ is the GLYMO and PEG/arginine groups decomposing under increasing temperature, both MNPs plateau and stabilise from 420°C . The citrate-MNPs also have a two-step weight loss, the initial weight loss is due to the evaporation of water between $80\text{--}120^\circ\text{C}$. However, coordinated water, which is a characteristic of citrate bound to the iron oxide core, has a higher boiling point than uncoordinated water⁴ as seen in the continued weight loss of 170°C . The citrate is seen to decompose at 300°C in the second region of weight loss. At

420°C there is some small interference which causes the weight to fluctuate across a 5°C range, this is due to instrumental error and it corrects itself at 407°C.

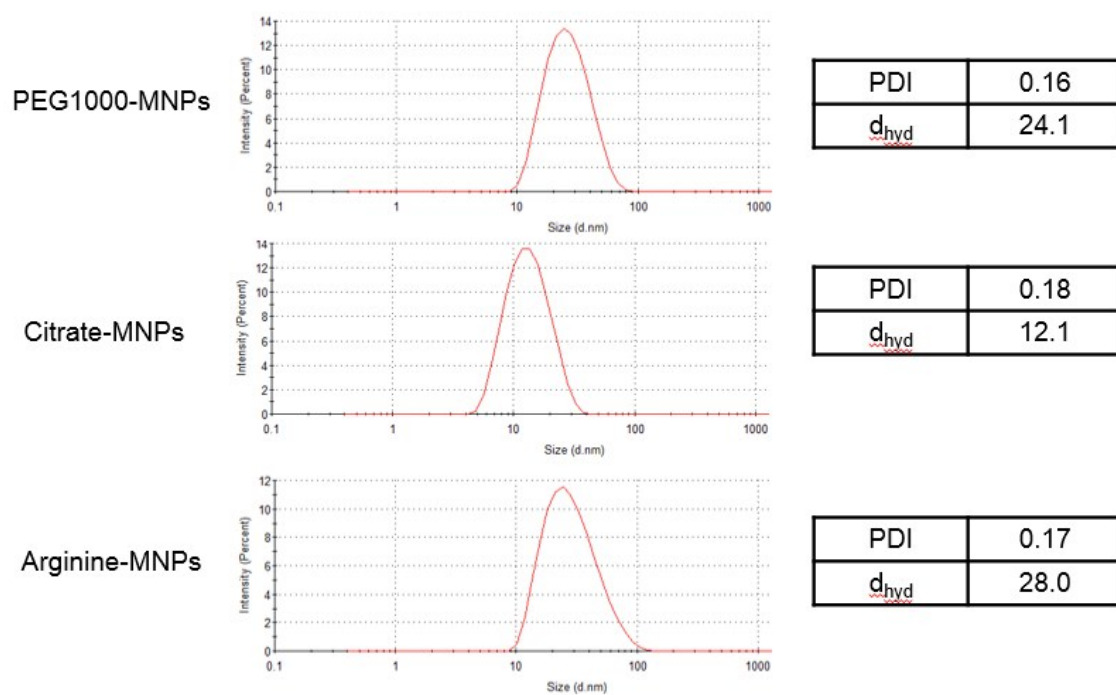


Figure S5 DLS size distributions for PEG1000-, arginine- and citrate-MNPs in H₂O at 298 K.

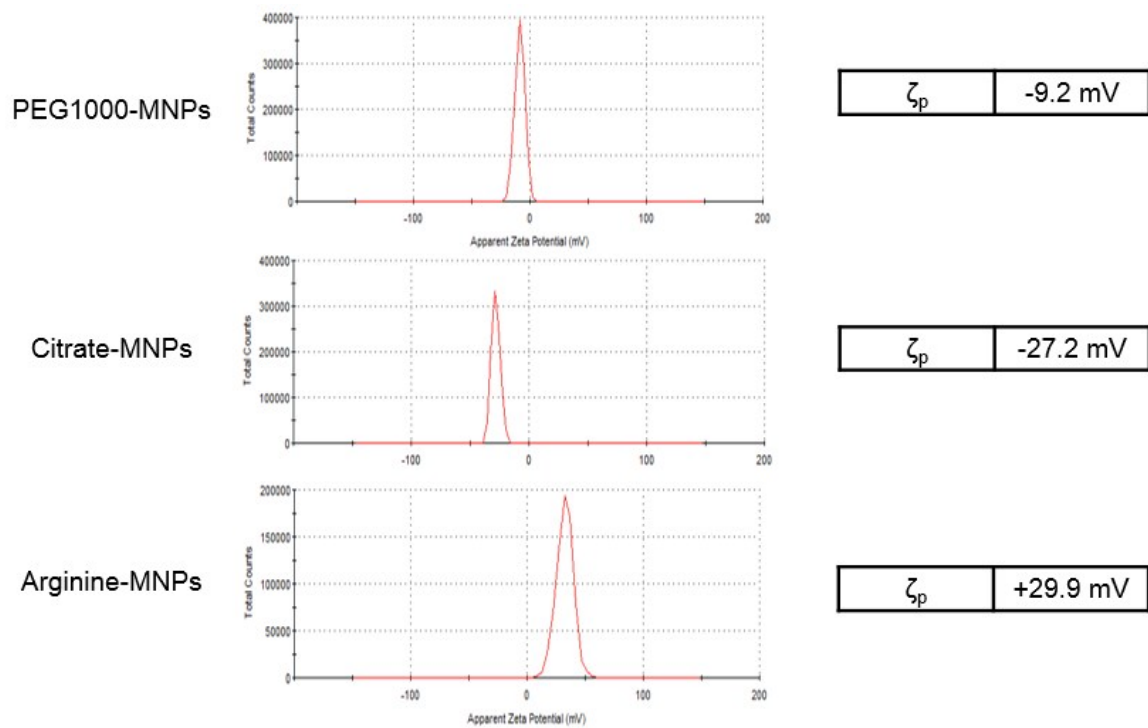


Figure S6 Zeta distributions for PEG1000-, arginine- and citrate-MNPs in H₂O at 298 K for PEG1000-, arginine- and citrate-MNPs measured by DLS in capillary folded cells. The measured ζ_p values are included.

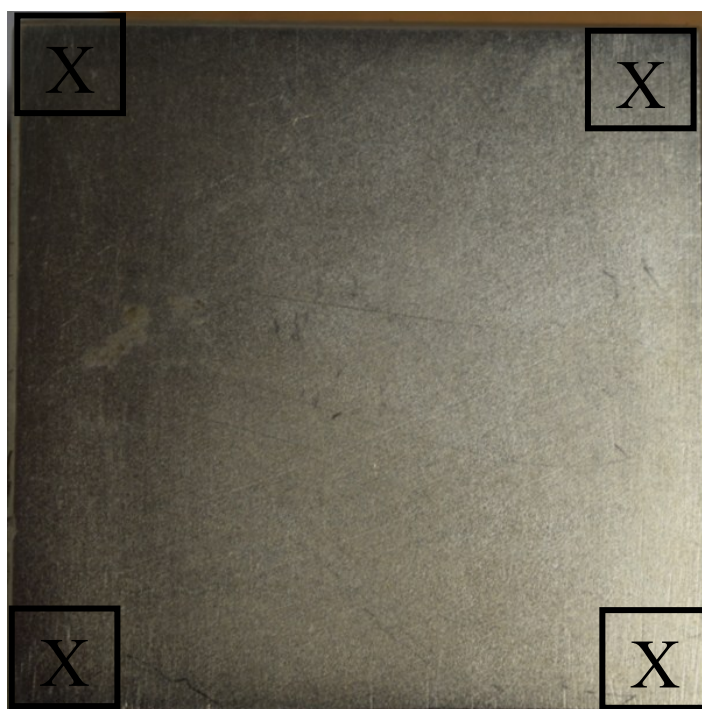


Figure S7 The magnetic force was found to be strongest and equivalent at the 4 corners of the magnet. The X above marks the positions used for the glass vial. It was found that the response was identical in all four positions.

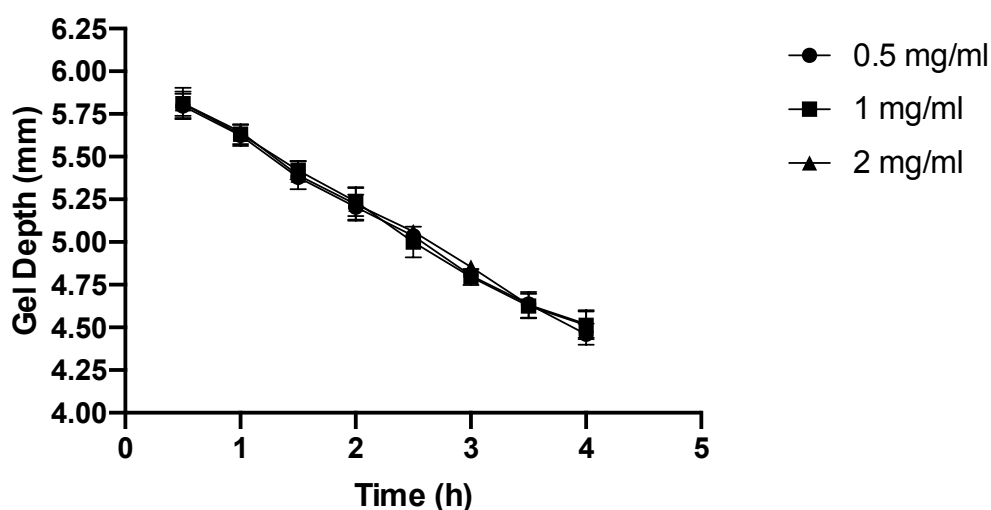


Figure S8 Magnetophoretic transport of ~ 1.0 mg/mL PEG1000-MNPs (d_{hyd} 24.0 nm, PDI 0.17) in aqueous suspension through agarose gel (0.3% w/v, low EEO) as a function of time ($n=4$). This experimental result demonstrates that (in this range) the concentration of the MNP solution used does not affect v_{exp} , suggesting that the MNPs move independently of each other.

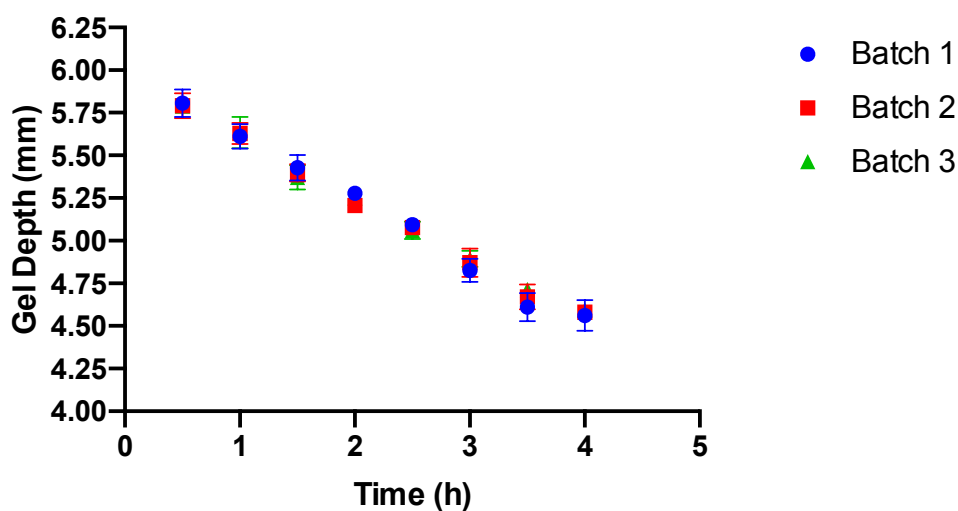


Figure S9 Magnetophoretic transport of 1.0 mg/mL PEG1000-MNPs (d_{hyd} 24.0 nm (0.17)) in aqueous suspension through agarose gel (0.3% w/v, low EEO) as a function of time ($n=4$). The consistent v_{exp} obtained by the PEG1000-MNPs demonstrates batch to batch reproducibility for three independent syntheses.

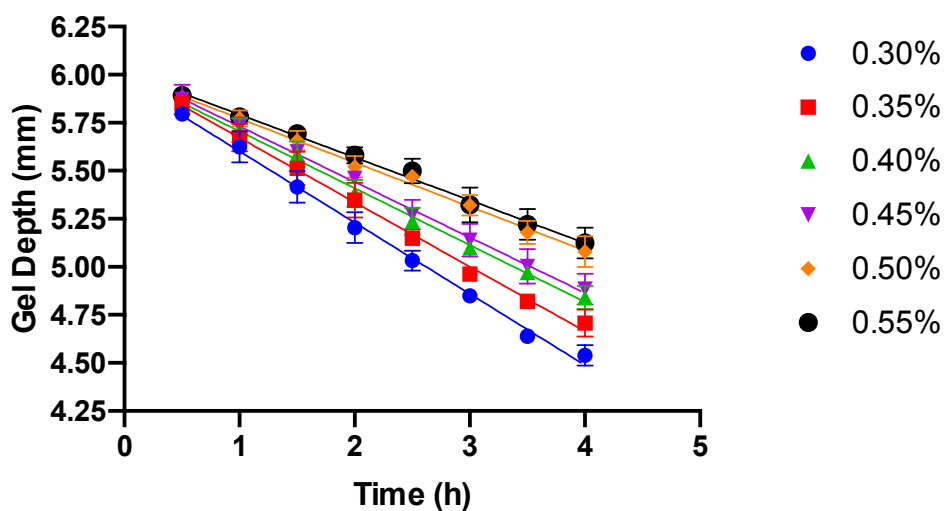


Figure S10 Magnetophoretic transport of ~ 1.0 mg/mL PEG1000-MNPs (d_{hyd} 24.0 nm, PDI 0.17) in aqueous suspension agarose gels with different agarose concentrations (0.30 - 0.55% w/v, low EEO). The excellent linear fits confirm that the PEG1000-MNPs attain a terminal velocity in each case and that v_{exp} decreases with increasing agarose content.

Agarose (% w/v)	Viscosity (Pa.s)
0.3	3080±112
0.35	3581±156
0.4	4201±201
0.45	4737±174
0.5	5340±245
0.55	5811±321

Figure S11 Tabulated data showing the measured viscosity values for the unloaded agarose gel samples over a range of concentrations.

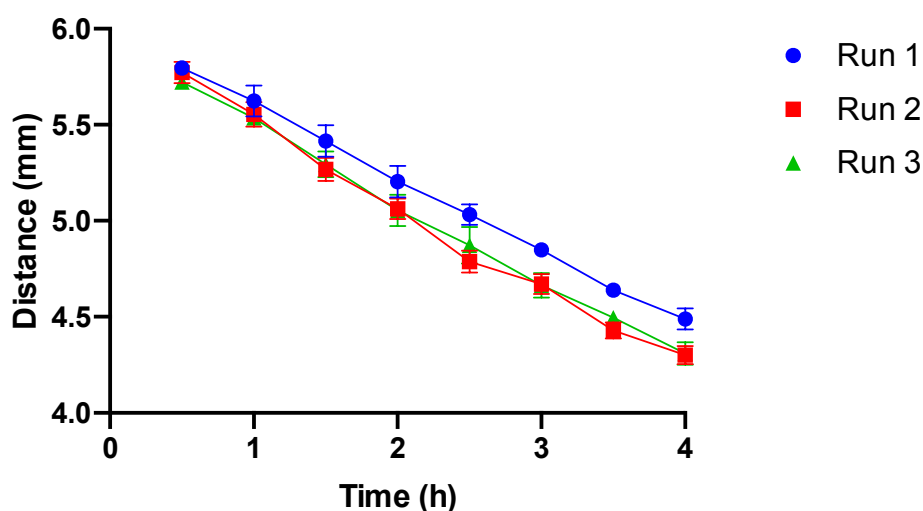


Figure S12 Magnetophoretic transport of ~ 1.0 mg/mL PEG1000-MNPs (d_{hyd} 24.0 nm, PDI 0.17) in aqueous suspension through agarose gel (0.3% w/v, low EEO). The MNPs were then extracted and the gel was re-loaded with a fresh aliquot of the same MNP suspension, and this process was repeated. This suggests that the passage of the front has little (if any) effect. The consistent V_{exp} over the three runs demonstrates that passage of the front has little (if any) effect on the gel, *i.e.* no damage is caused to the gel.

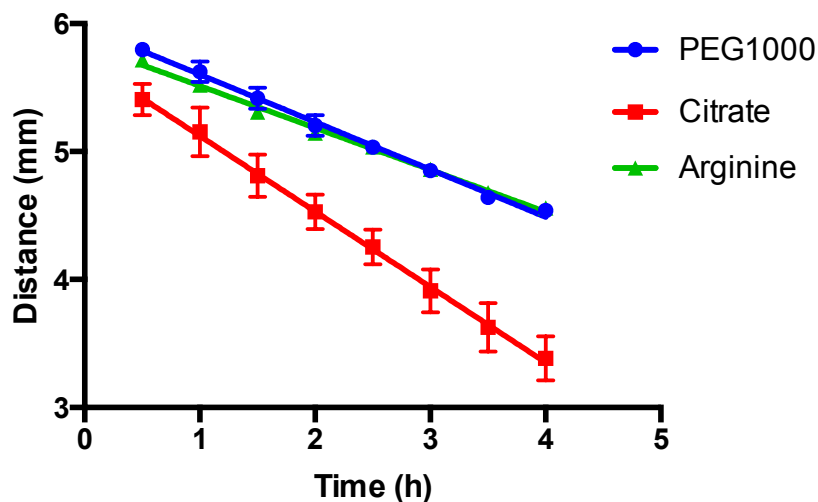


Figure S13 Magnetophoretic transport for PEG1000-, citrate- and arginine-MNPs in aqueous suspension through agarose gel (0.3% w/v, low EEO). Data is linear for all MNPs demonstrating velocities are constant during transit which provides evidence that the MNPs are not being damaged as they move through and interact with the viscous medium.

Surface chemistry	Before transit through agarose		After transit through agarose	
	d_{hyd} (nm)	ζ_p (mV)	d_{hyd} (nm)	ζ_p (mV)
PEG1000-	24.1	-9.3	24.0	-9.2
Citrate-	12.2	-27.2	12.1	-27.1
Arginine-	28.0	+30.1	28.0	+29.9

Figure S14 DLS measurements for PEG1000-, citrate- and arginine-MNPs suspensions before and after transit through the agarose gel. The consistent values for size and charge would indicate that the MNPs are not damaged in transit and remain stable.

Surface chemistry	d_{hyd}	d_{hyd}	d_{hyd}	d_{hyd}
-------------------	------------------	------------------	------------------	------------------

	IS – 0 (nm)	IS – 0.001 (nm)	IS – 0.005 (nm)	IS – 0.01 (nm)
PEG1000	24.0	24.0	24.1	24.1
Citrate	12.0	12.0	12.2	12.3
Arginine	28.0	28.0	28.1	28.2

Figure S15 DLS measurements for MNP suspension as a function of ionic strength, IS.

IS	Agarose class (EEO)	v_{exp} (mm/h)	v_{th} (mm/h)	%D
Low (0.001)	Low	0.63 (0.01)	0.75 (0.01*)	-19
High (0.01)	Low	0.66 (0.02)	0.75 (0.01*)	-12
Low (0.001)	High	0.65 (0.01)	0.75 (0.01*)	-13.3
High (0.01)	High	0.68 (0.01)	0.75 (0.01*)	-9.3

Figure S16 Magnetophoretic parameters for transport of ~1 mg/mL citrate-MNP suspension in aqueous buffered media of varying IS through agarose gels (0.3% w/v) of different EEO levels.

References:

1. Kuhn, S. J., Hallahan, D. E. & Giorgio, T. D. Characterization of superparamagnetic nanoparticle interactions with extracellular matrix in an in vitro system. *Ann. Biomed. Eng.*, 2006, **34**, 51–58.
2. Ninjbadgar, T. & Brougham, D. F. Epoxy ring opening phase transfer as a general route to water dispersible superparamagnetic Fe₃O₄ nanoparticles and their application as positive MRI contrast agents. *Adv. Funct. Mater.*, 2011, **21**, 4769–4775.
3. Benoit, D.N., Zhu, H., Lillierose M.H., Verm, R.A., Ali, N., Morrison, A.N., Fortner, J.D., Avendano, C., and Colvin, V.L. Measuring the grafting density of nanoparticles in solution by analytical ultracentrifugation and total organic carbon analysis. *Anal. Chem.*, 2012, **21**, 9238-9245.
4. Salazar-Medina, A.J., Gamez-Corrales, R., Ramirez, J.Z., Gonzalez-Aguilar, G.A., & Velazquez-Contreras, E.F. Characterization of metal-bound water in bioactive Fe (III)-cyclophane complexes. *J. Mol. Struct.*, 2018, **1154**, 225-231.